Modelica Component Models for Oceanic Surface Waves and Depth Varying Current

Savin Viswanathan[1] Christian Holden[1]

[1]Dept. of Mechanical and Industrial Engineering, Norwegian University of Science and Technology (NTNU), NO-7491 Trondheim, Norway. {savin.viswanathan,christian.holden}@ntnu.no

Abstract

In this paper, the theory of progressive ocean-surface gravity-waves is discussed, followed by the concept of the representation of the irregular sea-state by a sea-spectrum. Fourier series decomposition of the irregular sea-surface into its constituent regular waves and the method of realizing unique time-records of the sea-surface-elevation from commonly used sea-spectra is described. A detailed description of the development of *Modelica* component-models to generate regular as well as irregular waves, and depth-varying current, with an eye on the requirements imposed by probable integrated simulation scenarios, is then presented and the results discussed.

Keywords: regular wave, irregular wave, sea-spectrum, Modelica ocean-engineering library.

1 Introduction

The advantages of developing an *OpenModelica* ocean engineering library populated with domain-specific *component-models* and *functions* to carry out the integrated simulation of multi-pyhsical ocean engineering systems was demonstrated by the authors (Viswanathan and Holden, 2019). This earlier work:

1. Gives a brief description of the simulation of systems based on the hydrodynamic response of catenary-moored non-diffracting floating objects in the presence of waves and current,

2. Demonstrates the satisfactory agreement of the *Modelica* simulation results with those obtained using a popular ocean-engineering commercial software (*Orcaflex*), and

3. Brings out the advantages of using a component-model based simulation approach.

The voluminous nature of the earlier work precluded the possibility of delving into the theoretical and implementational details of the various *Modelica* component-models of the ocean-engineering library proposed by the authors, the preliminary version of which is available for download at `github.com/Savin-Viswanathan/OELib_OMAE2019`.

The present work which deals with the development of *Modelica* component-models for simulating the kinematics and dynamics of regular and irregular waves, and depth varying current, is the first among a series of two papers which will fill in such gaps in theory and implementation.

2 Theory

The theory presented here upto Section 2.4.2 is a brief summary of that given in (Dean and Dalrymple, 2001) .

2.1 The Fundamentals

The application of the conservation of mass to a reference fluid volume yields the continuity equation:

$$\frac{1}{\rho}\left(\frac{\partial\rho}{\partial t}+u\frac{\partial\rho}{\partial x}+v\frac{\partial\rho}{\partial y}+w\frac{\partial\rho}{\partial z}\right)+\frac{\partial u}{\partial x}+\frac{\partial v}{\partial y}+\frac{\partial w}{\partial z}=0. \tag{1}$$

Here, ρ [kg/m^3] is the fluid density, t [s] is time, and u,v,w [m/s] are the fluid velocities in the x,y,z directions.

Disregarding the effects of surface tension and elasticity, the application of the translational equation of motion to a fluid particle yields the Navier-Stoke's equations:

$$\frac{\mathrm{D}u}{\mathrm{D}t}=-\frac{1}{\rho}\frac{\partial p}{\partial x}+\frac{1}{\rho}\left(\frac{\partial\tau_{xx}}{\partial x}+\frac{\partial\tau_{yx}}{\partial y}+\frac{\partial\tau_{zx}}{\partial z}\right)+X, \tag{2}$$

$$\frac{\mathrm{D}v}{\mathrm{D}t}=-\frac{1}{\rho}\frac{\partial p}{\partial y}+\frac{1}{\rho}\left(\frac{\partial\tau_{xy}}{\partial x}+\frac{\partial\tau_{yy}}{\partial y}+\frac{\partial\tau_{zy}}{\partial z}\right)+Y, \tag{3}$$

$$\frac{\mathrm{D}w}{\mathrm{D}t}=-\frac{1}{\rho}\frac{\partial p}{\partial z}+\frac{1}{\rho}\left(\frac{\partial\tau_{xz}}{\partial x}+\frac{\partial\tau_{yz}}{\partial y}+\frac{\partial\tau_{zz}}{\partial z}\right)+Z. \tag{4}$$

Here, $\frac{\mathrm{D}}{\mathrm{D}t}$ is the material derivative, p [N/m^2] is the fluid pressure, τ [N/m^2] is the shear stress where the first subscript refers to the surface perpendicular and the second subscript refers to the direction of the stress, and X,Y,Z [N] are body forces along the x, y, and z directions.

2.2 Assumptions and the Governing Equation

The following assumptions are made:

- Incompressible fluid (ρ =constant).
- Inviscid fluid ($\tau = 0$).
- Irrotational flow ($\frac{\partial w}{\partial y}=\frac{\partial v}{\partial z}, \frac{\partial w}{\partial x}=\frac{\partial u}{\partial z}$ and $\frac{\partial v}{\partial x}=\frac{\partial u}{\partial y}$).

have been prepared with ocean engineers, most likely to be unfamiliar with *Modelica*, in mind, and some elements might appear super uous to the *Modelica* savvy reader.

3.2 Regular-Wave Component-Model

The height of the regular wave H_r [m], time period T_r [s], water depth d [m], water density $_w$ [kg/m^3], ramp time T_{rmp} [s], delay time T_{del} [s] and the number of frequency components $_n$ $_i$ 1 are speci ed as *parameters* in the **Regular_Airy_Wave** component model. T_{sim} [s] is the required duration of simulation.

T_{rmp} is used to ramp the wave height in order to prevent impulse wave loads at the start of the simulation, while T_{del} maybe used to start the waves at a speci ed time into the integrated simulation.

The wave angular frequency 2 T [rad] and d are passed on as parameters to the function **waveNumberIterator**, which iterates for the wave number based on the dispersion relation given in (31), and returns the nal value to **Regular_Airy_Wave**.

A data connector **WaveDataConnector** transmits d, $_w$, , T, k, , $_{0i}$, and SSE_{X0} to the data bus which is an *expandable connector* named the **EnvironmentBus**. Here, [rad], the phase difference is redundundant for the case of a regular wave and is set to zero, while SSE_{X0} is the sea surface elevation calculated at x 0 using (38).

The algorithm for generation of regular wave parameters is depicted in the ow chart given in Figure 5, and the ow chart for the *function* **waveNumberIterator** is given in gure 6. The rst value for the wave number iteration is taken to be k_0 $\frac{2}{L_0}$, where L_0 $\frac{gT^2}{2}$ [m] is the deep-water wave length as given on p. 66 of (Dean and Dalrymple, 2001).

Equations (37) (45) can then be used to calculate the wave properties at the required position coordinates, contained in the body component-model, at any required simulation time t [s].

3.3 Irregular-Wave Component-Model

The generation of component wave parameters based on the Pierson-Moskowitz spectrum is considered for detailed description. The algorithm for the irregular-wave component-model **IRW_PM_RDFCWI** is shown in Figure 7.

The water depth d [m], signi cant wave height H_s [m], the ramp time T_{rmp} [s], the lower cut-off frequency $_{min}$ [rad/s], the upper cut-off frequency $_{max}$ [rad/s], and the number of frequency components to be considered $_n$ $_i$, are speci ed as *parameter* inputs.

The frequency resolution Δ $_{max}$ − $_{min}$ $_n$ $_i$ [rad/s] is determined. The component frequency within each frequency interval Δ is then selected based on a uniform random distribution by the *function* **frequencySelector**.

To generate a vector of random numbers, a *function* **randomNumberGenerator** based on the *Modelica.Math.Random.Generators.Xorshift64star* random

Figure 5. Flow chart for regular-wave component-model.

number generator, with a *for* loop included, to return a vector of random numbers of specified size, corresponding to the number of frequency components $_n\omega_i$, is called. The **frequencySelector** function is a simple function that shifts the component frequencies randomly within the associated frequency interval based on the generated random numbers $rnd\_shft[_n\omega_i]$.

Once the component frequencies are identified, the corresponding spectral values are determined by calling the *function* **spectrumGenerator_PM** which calculates the

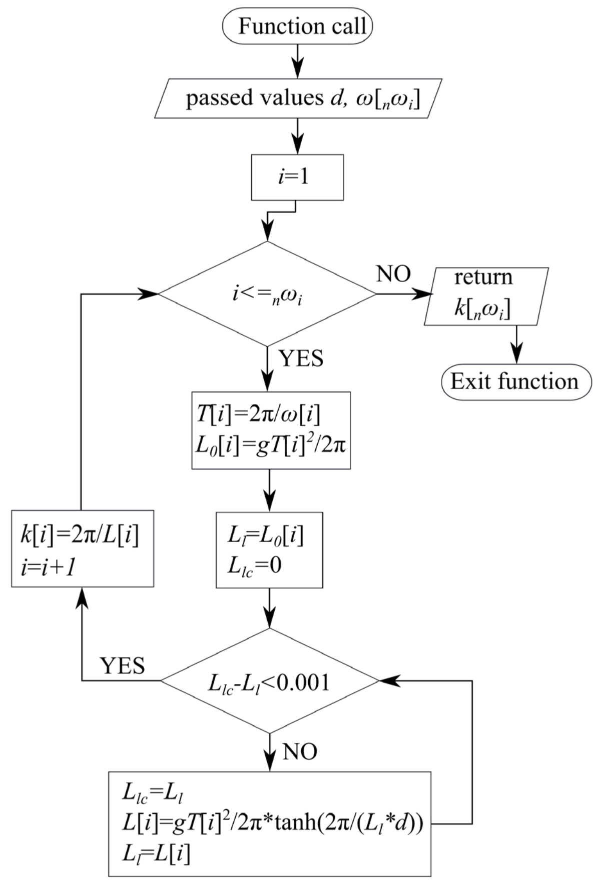

Figure 6. Flow chart for iteration of the wave number.

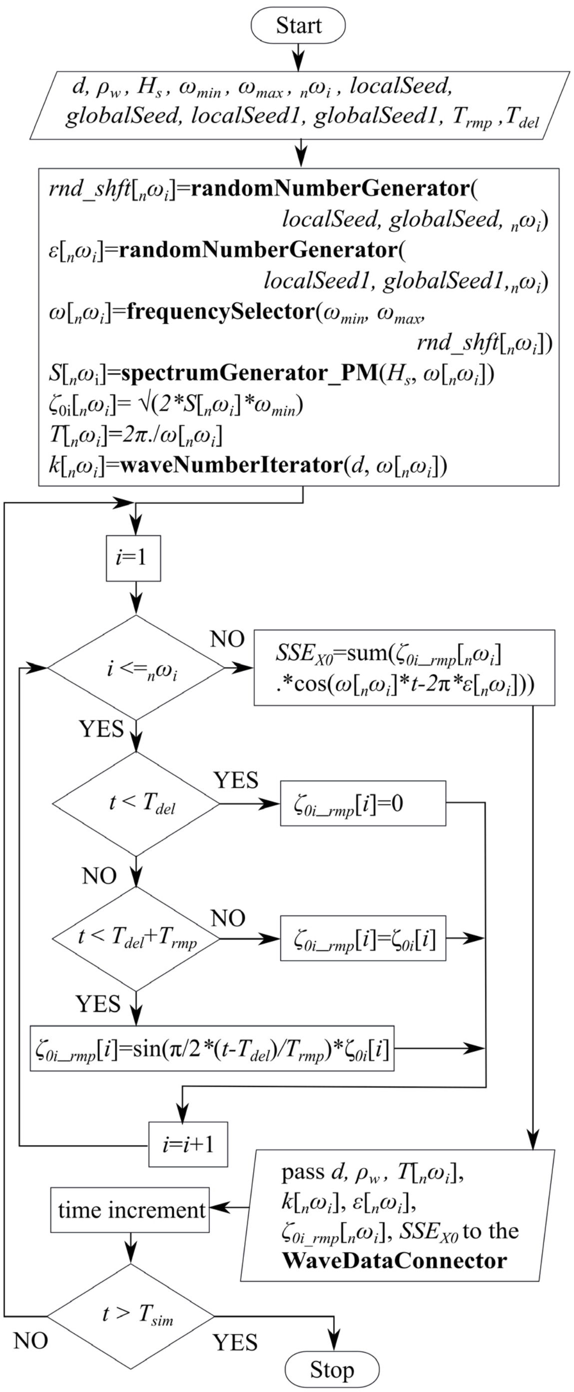

Figure 7. Flow chart for the irregular-wave component-model.

spectral density values based on the empirical formula

$$S_\eta(\omega_i) = \frac{5\pi^4 H_s^2}{T_p^4 \omega_i^5} \exp\left(\frac{-20\pi^4}{T_p^4 \omega_i}\right). \tag{49}$$

Here, T_p [s] is the peak period of the spectrum, and is related to H_s through the relations $T_p = \frac{2\pi}{\omega_p}$, and $\omega_p^2 = \frac{0.161g}{H_s}$. ω_p [rad/s] is the peak angular frequency; see pp. 105–107 of (Chakrabarti, 1987).

In the future, generation of wave records based on other commonly used sea-spectra may be incorporated by defining the correspoding spectrum generating functions.

The amplitudes of the component waves ζ_{0i} are then determined using (47), and corresponding wave numbers k_i are determined using the *function* **waveNumberIterator** described in Section 3.2. The randomly distributed phases are determined by a second call to the *function* **randomNumberGenerator**. This function call returns a vector $\varepsilon[{}_n\omega_i]$ of uniformly distributed random numbers in (0,1] and hence, the associated phase difference is expressed as $2\pi\varepsilon$ [rad] .

Having determined all the required parameters, the sea surface elevation at $x = 0$, SSE_{X0} [m], is then calculated using the formula given in (48). The values are then linked to the *expandable connector* EnvironmentBus using the **WaveDataConnector** as described in Section 3.2.

3.4 Component-Model of Depth-Varying Current

The component-model for current is a simple block which produces as its output two vectors $zcg[n]$ and $Ucg[n]$. zcg contains the co-ordinate information and Ucg contains the corresponding current velocities. The *parameters* specified are the $zcg[n]$ which is a vector containing the n depth positions where current velocities are defined, $Uf[n]$ which is a vector containing the fully developed current values, and the ramp time T_{rmp} [s]. $Ucg[n]$ holds the instantaneous value of the ramped current. A sinusoidal ramping function is used for smooth ramping. A **CurrentDataConnector** links the zcg and Ucg values to the *expandable connector* **EnvironmentBus**. The current velocity at any location may now be computed by the different body component-models by interpolation.

4 Results

All results presented below are based on outputs of the above component models. Simulation files are available for download at `github.com/Savin-Viswanathan/Modelica2020-a`.

4.1 Regular Wave

The simulation model **Check_RegularWave** under the *sample simulations* in the above link calculates the wave properties based on the parameters generated by the **Regular_Airy_Wave** component-model.

Figure 8a shows a sample sea surface elevation at $x = 0$ [m] with $T_{del} = 5$ [s], $T_{rmp} = 10$ [s], $H_r = 1$ [m], $d = 10$ [m] and $T_r = 3$ [s], for a simulation interval of 0–30 [s], while Figure 8b shows the progressive wave profile for the same wave in the spatial interval 0–30 [m] for different simulation times.

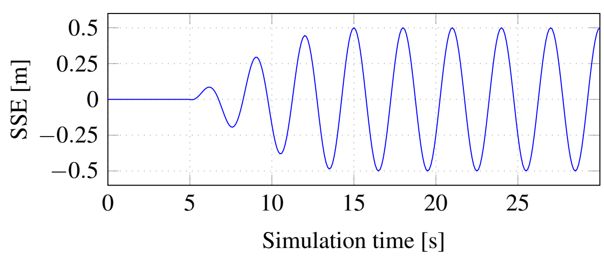

(a) Sea surface elevation at $x = 0$ for $t = [0, 30]$ s.

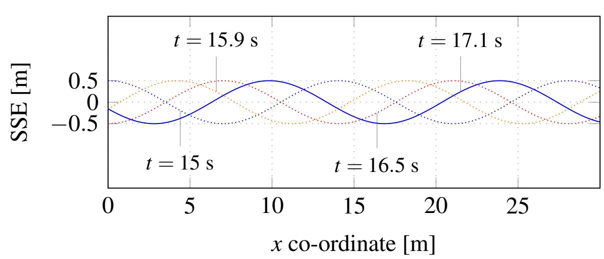

(b) Wave profile at different simulation time steps for $x = [0, 30]$ m.

Figure 8. Sea surface elevation and the progressive wave profile.

Figure 9a shows the wave profiles at $t = 0$ [s] for different T_r, and Figure 9b shows the trajectory traced by water particles with different mean positions during a complete wave cycle, at different depths, for the different wave periods, in a water depth $d = 10$ [m]. We observe that,

- For $T_r = 3$ [s], $k = 0.447414$ [m^{-1}], and $kd > \pi$. The wave is in *deep water* and the trajectories are circular. The displacements in the vertical and horizontal directions decay exponentially with depth and the particles near the bottom boundary have no horizonatal or vertical displacements.
- For $T_r = 6$ [s], $k = 0.129834$ [m^{-1}], and $\frac{\pi}{10} < kd < \pi$. The wave is in *intermediate water* and the trajectories are elliptical. The displacements in the vertical and horizontal directions decay with depth and the particles near the bottom boundary have only horizontal displacements.
- For $T_r = 22$ [s], $k = 0.029246$ [m^{-1}], and $kd < \frac{\pi}{10}$. The wave is in *shallow water* and the trajectories are elliptical. The displacements in the vertical direction decay linearly with depth, while the horizontal displacement is near constant at all depths.

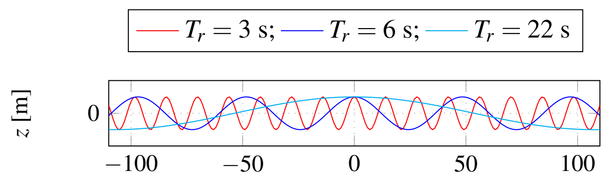

(a) Profiles of waves with different periods.

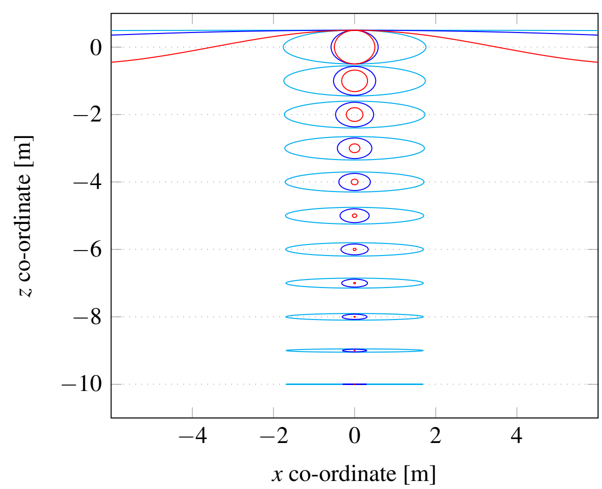

(b) Water particle trajectories of waves with different wave periods.

Figure 9. Wave profiles and water particle trajectories.

Figure 10a shows the intstantaneous wave profile for a regular progressive wave with $T_r = 6$ [s], $H_r = 1$ [m], in a water depth $d = 10$ [m], when there is a crest at $x = 0$ [m]. Figure 10b–10f shows the quiver plots for the instantaneous velocities of water-particles with different mean z co-ordinates, under different x co-ordinates.

An important consideration to keep in mind is that the linearization of the boundary conditions in the derviation of the velocity potential has the effect that the water particle kinematics derived from such a potential does not

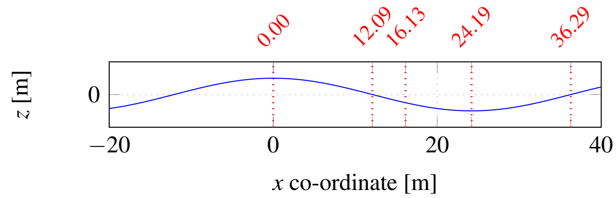

(a) Wave profile and x co-ordinates where the velocities are measured

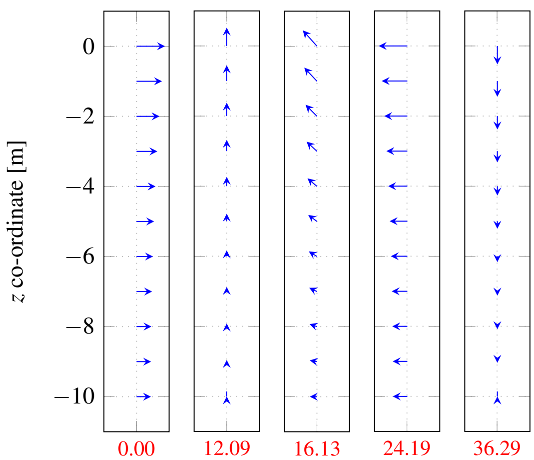

(b) **(c)** **(d)** **(e)** **(f)**

Figure 10. Wave profile (a), water-particle velocities (b)–(f).

account for the change of position of the particle within the fluid, and hence the theory cannot give a proper description for flow velocity and acceleration in the region between the still water level and the wave crest and in the void to the wave trough. Extrapolation of the values is, in general, not recommended since the wave forces will be overestimated. A better way is to apply *Wheeler stretching* or *move* the profile for velocity and acceleration to the instantaneous sea surface; see p. 221 of (SINTEF, 2014).

Figure 11 shows the pressure distribution at various x co-ordinates for the same wave as above. The dynamic pressure above $z = 0$ [m] has been calculated using a truncated Taylor series for small positive distances, as given on p. 84 of (Dean and Dalrymple, 2001).

4.2 Irregular Wave

Figure 12a depicts a Pierson-Moskowitz spectrum of $H_s = 1$ [m] generated by the **spectrumGenerator_PM** function, while Figure 12b depicts the sea surface elevation for an irregular wave record with 100 frequency components, generated from the spectrum by the **IRW_PM_RDFCWI** irregular-wave component-model with $T_{rmp} = 10$ [s], $T_{del} = 0$ [s], $\Delta\omega = \omega_{min} = 0.03141$ [rad/s], and $\omega_{max} = 3.141$ [rad/s]. Figure 12c shows an expanded view of the same wave record in a shorter time interval, for clarity.

4.3 Depth-varying Current

Figure 13 depicts the instantaneous profile for a depth varying current which is based on the output of the **CurrentProfile_4pt** component-model. The current is ramped up to full value using the parameter $T_{rmp} = 5$ [s].

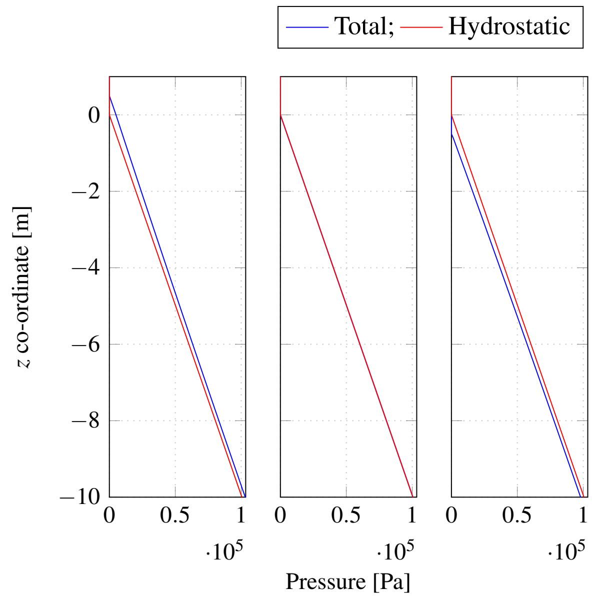

(a) $x = 0$ m **(b)** $x = 12.09$ m **(c)** $x = 24.19$ m

Figure 11. Pressures beneath the wave crest, down-crossing, and trough.

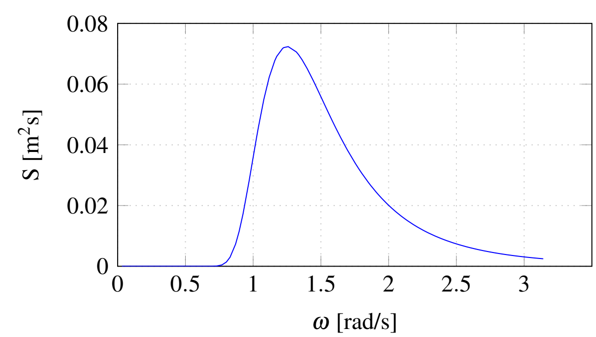

(a) Pierson-Moskowitz spectrum with $H_s = 1$ m.

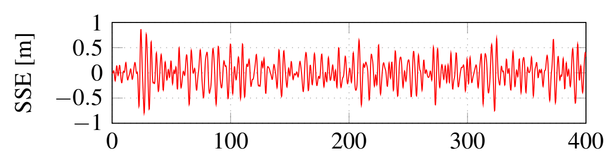

(b) SSE at $x = 0$ m for time interval [0, 400] s.

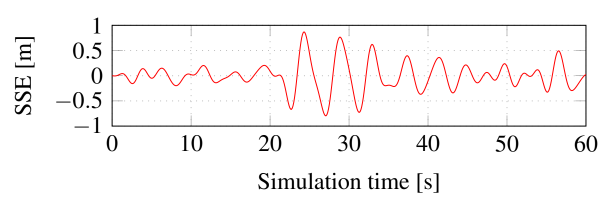

(c) SSE at $x = 0$ m for time interval [0, 60] s.

Figure 12. Irregular waves.

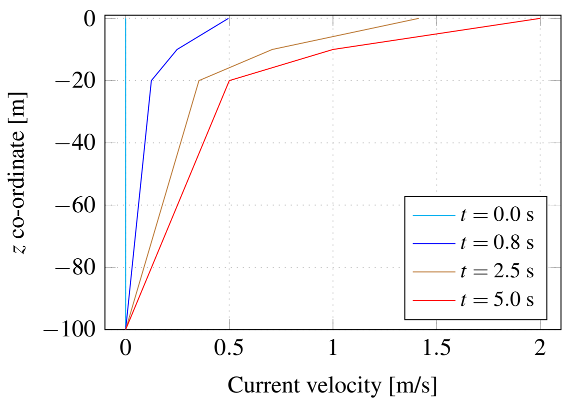

Figure 13. Current profile

5 Conclusion

General considerations to be kept in mind while formulating a framework for carrying out integrated simulation of ocean-engineering systems is presented and the algorithms for development of *Modelica* component-models for the generation of regular and irregular waves are described. The implementation of a simple component-model for generation of depth varying current is also presented.

Graphical representation of the wave kinematics and dynamics based on the output of the component-models for regular waves are then presented to show satisfactory agreement with general results discussed in (Dean and Dalrymple, 2001). A sample sea-surface-elevation based on the output of the component-model for irregular waves is presented. Since, within the assumption of linearity, the properties of the irregular wave are a linear combination of the properties of the consitutent regular waves, it is deemed that the output of the irregular wave component-model is satisfactory. Graphical representation of the output of the component-model for depth varying current is then presented.

For a better understanding of how these component models perform within an integrated simulation scenario, readers may refer to (Viswanathan and Holden, 2019). The present paper fills in for the lack of theoretical and implementational details for the wave and current component-models in the above work.

Theory and implementation of component-models for non-diffracting floating objects and for mooring forces based on the quasi-static catenary approach, used in (Viswanathan and Holden, 2019), is discussed in (Viswanathan and Holden, 2020), along with comparison of results for the same system modelled in the commonly used ocean-engineering software Orcaflex. Satisfactory agreement of surge/heave responses, and of Morison forces under various combinations of wave and current loading is demonstrated in (Viswanathan and Holden, 2020), and these maybe taken as proof for the correct representation of wave-current kinematics by the component models discussed in this work.

6 Acknowledgements

The research in this paper has received funding from the Research Council of Norway, SFI Offshore Mechatronics, project number 90034210.

References

Thomas Lykke Andersen and Peter Bak Frigaard. *Lecture Notes for the Course in Water Wave Mechanics*. Department of Civil Engineering, Aalborg University. DCE Lecture notes, No.24, 2011. URL vbn.aau.dk/en/publications/lecture-notes-for-the-course-in-water-wave-mechanics(69731932-7a17-47ea-b557-6b9e0c81050f).html.

Subratha Kumar Chakrabarti. *Hydrodynamics of Offshore Structures*. Computational Mechanics Publications, and Springer-Verlag, Dorchester, Great Britain, 1987. ISBN 0-905451-66-X.

Robert G. Dean and Robert A. Dalrymple. *Water Wave Mechanics for Engineers and Scientists*. Allied Publishers Limited, Mumbai, India, 2001. ISBN 81-7764-195-6.

Odd M. Faltinsen. *Sea Loads on Ships and Offshore Structures*. Cambridge University Press, 1999. ISBN 0-521-45870-6.

Thor I. Fossen. *Handbook of Marine Craft Hydrodynamics and Motion Control*. John Wiley & Sons, Chichester, United Kingdom, 2011. ISBN 97-8111-999-1496.

Harald E. Krogstad and Oivind A. Arntsen. *Lecture Notes on Linear Wave Theory- Part A- Regular Waves*. Norwegian University of Science and Technology, Trondheim, February 2000. URL folk.ntnu.no/oivarn/hercules_ntnu/LWTcourse/.

SINTEF. *Handbook on Design and Operation of Flexible Pipes*. 2014. URL sintef.no/en/latest-news/updated-handbook-on-design-and-operation-of-flexible-pipes/.

Alexandra H. Techet. *Free Surface Waves- Handout*. Massachusetts Institute of Technology, 2005. URL web.mit.edu/2.016/www/handouts/Free-Surface-Waves.pdf.

Savin Viswanathan and Christian Holden. Towards the development of an ocean engineering library for openmodelica. In *Proceedings of the ASME 2019 38th International Conference on Ocean, Offshore and Arctic Engineering.*, volume 7B: Ocean Engineering, OMAE2019-95054, June, 2019. URL doi.org/10.1115/OMAE2019-95054.

Savin Viswanathan and Christian Holden. Modelica component-models for non-diffracting floating objects and quasi-static catenary moorings. *Proceedings of the American Modelica Conference*, March, 2020. The referring paper and the referred paper are part of the proceedings of the same conference.